Theoretical investigation of atomic and electronic structures of $Ga_2O_3(ZnO)_6$

Juarez L. F. Da Silva,[1,2] Aron Walsh,[3] and Su-Huai Wei[1]
[1]*National Renewable Energy Laboratory, 1617 Cole Boulevard, Golden, Colorado 80401, USA*
[2]*Instituto de Física de São Carlos, Universidade de São Paulo, Caixa Postal 369, São Carlos 13560-970, SP, Brazil*
[3]*Department of Chemistry, Materials Chemistry, University College London, London WC1H 0AJ, United Kingdom*
(Received 10 August 2009; revised manuscript received 17 November 2009; published 29 December 2009)

Transparent conducting oxides (TCO) are widely used in technological applications ranging from photovoltaics to thin-film transparent field-effect transistors. In this work we report a first-principles investigation, based on density-functional theory, of the atomic and electronic properties of $Ga_2O_3(ZnO)_6$ (GZO_6), which is a promising candidate to be used as host oxide for wide band gap TCO applications. We identify a low-energy configuration for the coherent distribution of the Ga and Zn atoms in the cation positions within the experimentally reported orthorhombic GZO_6 structure. Four Ga atoms are located in four-fold sites, while the remaining 12 Ga atoms in the unit cell form four shared Ga agglomerates (a motif of four atoms). The Zn atoms are distributed in the remaining cation sites with effective coordination numbers from 3.90 to 4.50. Furthermore, we identify the natural formation of twin-boundaries in GZO_6, which can explain the zigzag modulations observed experimentally by high-resolution transmission electron microscopy in GZO_n ($n=9$). Due to the intrinsic twin-boundary formation, polarity inversion in the ZnO tetrahedrons is present which is facilitated by the formation of the Ga agglomerates. Our analysis shows that the formation of fourfold Ga sites and Ga agglomerates are stabilized by the electronic octet rule, while the distribution of Ga atoms and the formation of the twin-boundary help alleviate excess strain. Finally we identify that the electronic properties of GZO_6 are essentially determined by the electronic properties of ZnO, i.e., there are slight changes in the band gap and optical absorption properties.

DOI: 10.1103/PhysRevB.80.214118 PACS number(s): 61.43.−j, 61.50.Ks, 71.15.Nc

I. INTRODUCTION

Transparent conducting oxides (TCOs) are unusual materials. They are both transparent (with an average transmittance above 80% in the visible spectrum range) and conductive (with resistivity less than 10^{-3} Ω cm),[1–3] therefore, they are used in a wide range of technological applications such as solar cells, display panels, thin-film transparent field-effect transistors.[4–13] Although indium-oxide doped by tin (ITO), In_2O_3:Sn,[14] has been the TCO of choice in industrial applications, alternative host oxides, consisting of combination of two or more binary oxides such as In_2O_3, Ga_2O_3, Al_2O_3, SnO_2, ZnO, and CdO, have been investigated as to improve the material quality and reduce the cost by decreasing the amount of In.[15–18] These multiternary compounds can be synthesized either in the amorphous phase[19–23] or crystalline phases.[24–34] Recently, nanostructures of these oxides have also been reported,[35–38] which opens the possibility for technological applications. Among several reported multicompounds, the combination of Ga_2O_3 and ZnO $[Ga_2O_3(ZnO)_n]$ has been widely studied because it has a wide band gap and high stability, thus suitable for short wavelength applications.[5,39]

Crystalline $Ga_2O_3(ZnO)_n$ (GZO_n, n=integer) compounds can be synthesized by solid state reactions using stoichiometric proportions of Ga_2O_3 and ZnO and heated at high temperatures (about 1200–2000 K).[25,29,34,40,41] So far, compositions with $n=1$,[40,41] $n=6$,[34] $n=7,8,9,16$,[25] and $n=9,13$ (Ref. 29) have been reported. Experimental characterizations using x-ray diffraction (XRD) have found that GZO_n crystallizes in orthorhombic structures for $n>1$ and the cubic normal spinel structure for $n=1$. However, the internal structural parameters (atomic positions) have been reported only for $n=1$ and 6.[34] Thus, in contrast to the crystalline $In_2O_3(ZnO)_n$ (IZO_n) compound for which there are several available experimental[25,30,38,42–48] and theoretical[49–52] studies, GZO_n has not been well characterized, and hence, several questions remain open (see below).

Employing XRD, Michiue *et al.*[34] identified an orthorhombic structure for GZO_6, Fig. 1, in which the cations indicated by M are four- and five-fold coordinated with respect to the oxygen anions. It can be seen in Fig. 1 that the $M4$ and $M9$ cations form trigonal-bipyramidal structures with their neighbor oxygen atoms, while the remaining cations form tetrahedron structures such as Zn in the binary wurzite structure.[53] Almost all O atoms are four-fold coordinated with the cations, although some O atoms are threefold coordinated. It can be noticed in Fig. 1 that the $M7$ and $M8$ sites are very close to each other (1.70 Å), while most of the cations are separated by at least 3.10 Å, and hence, as pointed out by Michiue *et al.*, the $M7$ and $M8$ sites cannot be simultaneously occupied by two cations. Thus, the sum of the occupation of the $M7$ and $M8$ sites was fixed at unity in the XRD analysis. Because XRD cannot clearly distinguish between the Ga and Zn atoms as their atomic numbers differs only by one, it was assumed by Michiue *et al.* that the 16 Ga atoms occupy the $M4$ and $M9$ sites, and the Zn atoms occupy the remaining cation sites. These assumptions lead to the assignment of space group *Cmcm* for GZO_6, which is shown in Fig. 1.

The pioneering work reported by Michiue *et al.*[34] provided a basis for the understanding of the atomic structure of GZO_n compounds ($n>1$), but several questions still remain: Is there a preferential occupation of the $M7$ or $M8$ sites by Zn or Ga atoms? Is the trigonal bipyrimidal sites occupied

 ©2009 The American Physical Society

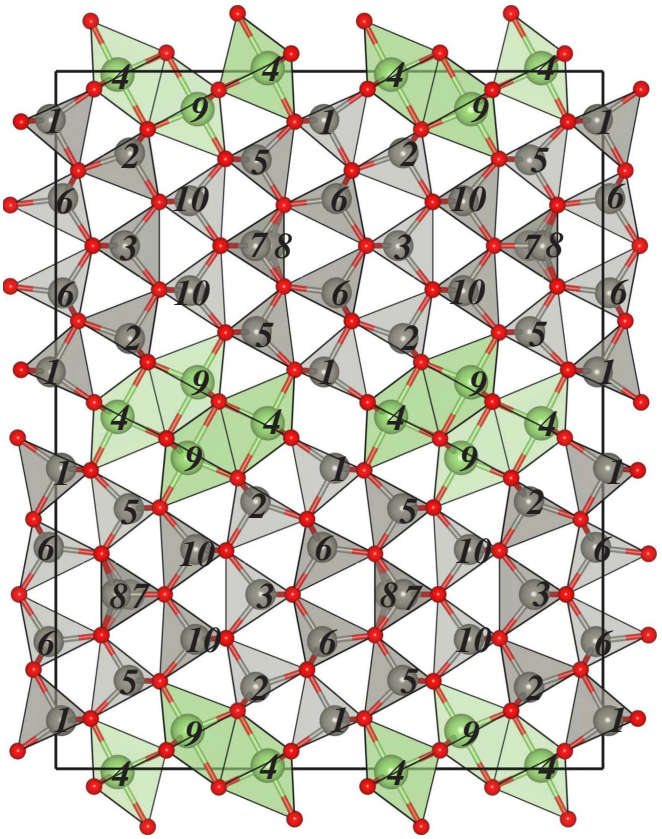

FIG. 1. (Color online) Atomic structure of the orthorhombic GZO_6 compound obtained by x-ray diffraction. (Ref. 34) All 10 nonequivalent cation sites M are indicated by numbers. The large (green), medium (brown), and small (red) balls denote Ga, Zn, and O atoms, respectively. The unit cell and polyhedrons are indicated as well.

only by Ga atoms? Is there a preference for a homogeneous distribution of the Ga atoms in the M sites or the formation of local Ga motifs is favored. To address these questions we have performed first-principles calculations based on density-functional theory (DFT). We identified the occupation of the cation sites by Ga and Zn atoms that leads to the lowest energy configurations, as well as the underlying mechanisms that lead to the structural stability. We show that the formation of a natural twin grain boundary in GZO_6 plays a similar role as the zigzag modulations in IZO_n to release stress energy.[51] Furthermore, we have also calculated the electronic properties of GZO_6 at its ground state structure. It is important to point out that although this study is performed only for $n=6$ and its parent compounds Ga_2O_3 and ZnO, the insights obtained in this study can be used to understand structural stability at other concentrations. The remainder of the paper is organized as follows: in Sec. II, the theoretical approach and computational details are described. in Sec. III, the structural, energetics, and electronic properties of GZO_6 are presented and discussed.

II. THEORETICAL APPROACH AND COMPUTATIONAL DETAILS

Our total energy calculations are performed using the all-electron projected augmented wave (PAW) method[54,55] and DFT (Refs. 56 and 57) within the generalized gradient approximation (GGA) formulated by Perdew, Burke, and Ernzerhof (PBE),[58] as implemented in the Vienna *ab initio* simulation package (VASP).[59,60] For Ga and Zn, the 3d states were included as valence electrons. Plane-wave cutoff energies of 400 and 800 eV were used for the total energy and stress tensor calculations, respectively, while for the Brillouin zone integration **k**-point grids of $(6\times1\times1)$ (four **k** points), $(2\times6\times4)$ (24 **k** points), and $(7\times7\times4)$ (24 **k** points) were used for the orthorhombic GZO_6, monoclinic β-Ga_2O_3, and wurtzite ZnO, i.e., all total energy and stress tensor calculations were performed using approximately the same **k** density for all systems.

The ground state total energies and equilibrium volumes for all structures were obtained by full relaxation of the volume, shape, and atomic positions (forces <0.01 eV/Å) of the unit cell to minimize the quantum mechanical stresses and forces. To obtain the electronic and optical properties, e.g., density of states and absorption coefficients, we employ higher **k** point densities, which is required to obtain smooth DOS and converged optical properties. For example, we employ 62, 616, and 1920 **k** points for GZO_6, β-Ga_2O_3, and ZnO, respectively. In order to obtain a better understanding of charge reorganization upon the multicompound formation, we employed Bader analysis within the implementation provided by Henkelman and co-workers,[61–63] which reads the total charge density calculated by VASP including the core electron density. For the Bader analysis, a denser double fast Fourier transformation mesh was used.

III. RESULTS AND DISCUSSION

A. Structural properties

In contrast to the IZO_n compounds, which crystallize in modulated-layered structures with hexagonal lattices,[25,28,30,50,51,64] GZO_6 has an orthorhombic structure with space group $Cmcm$.[25,29,34] Structures with the "V" shape modulations have also been reported for GZO_n,[29] however, their formation mechanism and the local structural arrangements are unclear. The experimental lattice constants obtained by XRD for GZO_6 are $a_0=3.25$ Å, $b_0=19.64$ Å, $c_0=24.78$ Å, and the unit cell contains 8 f.u. (16 Ga, 48 Zn, and 72 O atoms). However, as mentioned in the introduction, to determine the crystal structure, two assumptions were employed, namely, all Ga atoms occupy the bipyrimidal fivefold sites, while the $M7$ and $M8$ sites are fractionally occupied by Zn atoms. The remaining cation sites are occupied by Zn atoms.[34] In the $Cmcm$ structure, Fig. 1, the unit cell contains 7 sites ($M1$, $M2$, $M4$, $M5$, $M6$, $M9$, and $M10$), each has 8 equivalent positions. The other three sites ($M3$, $M7$, and $M8$), each have four equivalent positions. The $M7$ and $M8$ sites cannot be simultaneously occupied due to the short distance between both sites.

To search the atomic configuration of the lowest-energy structure, first, we assumed that all the 16 Ga atoms are distributed in the $M4$ and $M9$ sites as suggested by the XRD study,[34] while the remaining M sites are occupied by Zn atoms. We found that the occupation of the $M7$ sites [Fig. 2(c)] by Zn atoms is only 6 meV/f.u. lower in energy than

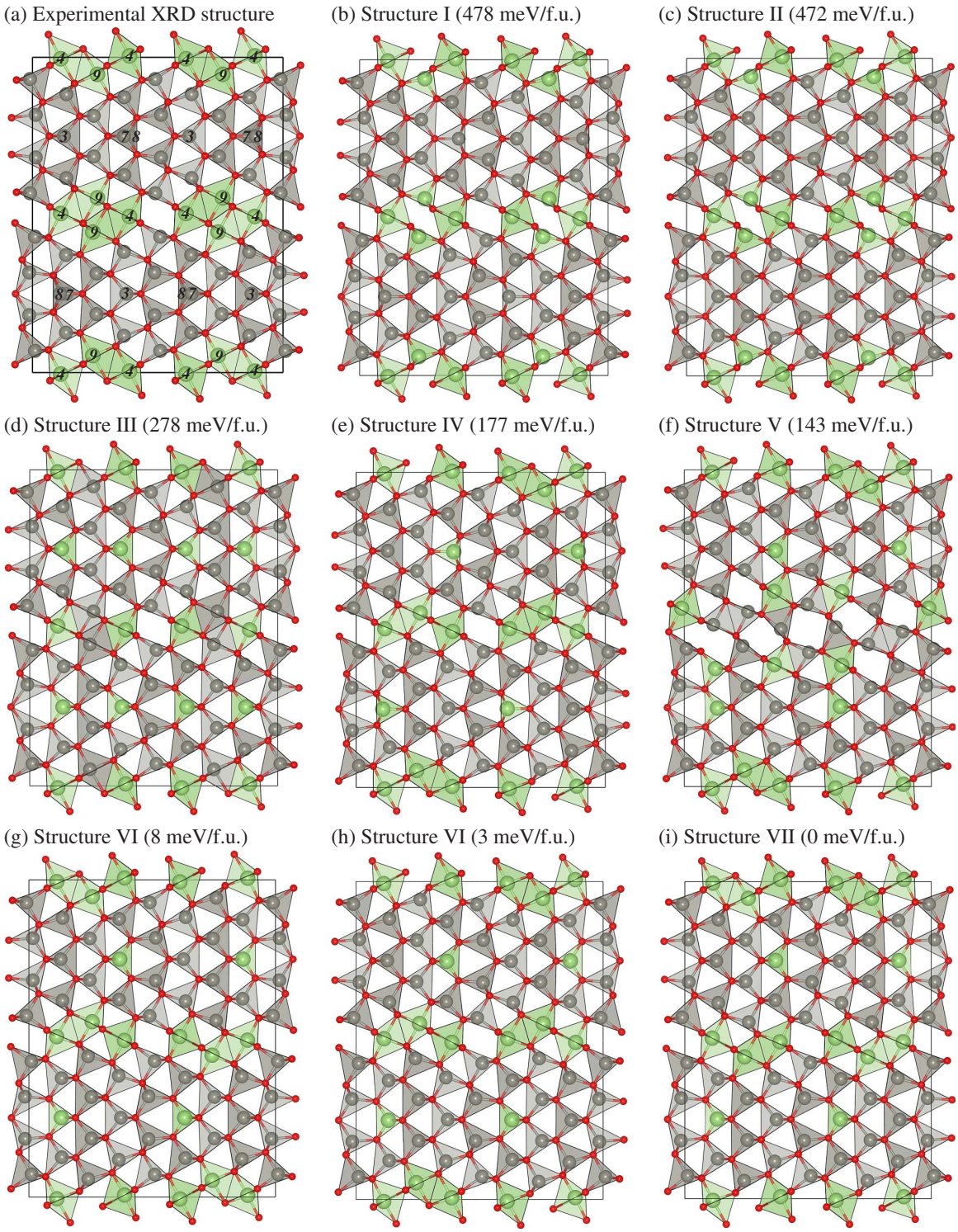

FIG. 2. (Color online) Structure models for the atomic distribution of the Ga and Zn atoms in the cation sites (M) of the orthorhombic GZO_6 structure. (a) Experimental XRD structure. (Ref. 34) The structure models shown in (b), (c), (d), (e), (f), (g), (h), and (i) have different distributions for the Ga and Zn atoms in the cation sites. The large (green), medium (brown), and small (red) balls indicate Ga, Zn, and O atoms, respectively. The relative total energies per f.u. are given with respect to the lowest energy structure (i), in which the Ga atoms occupy the $M4$, $M7$, and half of the $M9$ sites and Zn atoms occupy the remaining M sites.

the $M8$ sites [Fig. 2(b)]. Thus, due to the small energy difference, both sites might be occupied at room temperature by Zn atoms, which is consistent with the results reported by Michiue *et al.*[34]

A simple inspection of the coordination of the $M8$ and $M7$ sites indicates that they would not be energetically favorable to be occupied by Zn atoms because the resulting structures would not satisfy the electronic octet rule. For example, the

$M8$ and $M7$ sites are five- and four-fold coordinated, respectively. On the other hand, cations at $M8$ and $M7$ sites are surrounded by oxygen atoms with coordination equal or less than four. Thus, it implies that the occupation of $M8$ and $M7$ sites by Zn atoms cannot satisfy the electronic octet rule, which is known to play an important role to lower the crystal energy of multicomponent oxides.[51] In order to satisfy the electronic octet rule, the $M7$ sites should be occupied by cations with high valence, i.e., Ga atoms, while the $M8$ sites might be empty. In this case, two electrons are donated to the two three-fold O atoms, while the last electron is shared by the remaining two four-fold O atoms. In order to keep the *Cmcm* space group, the occupation of the $M7$ or $M8$ sites implies that the $M3$ sites should also be occupied by Ga, Fig. 2(d). However, this implies that the electronic octet rule for the Ga atoms at the $M3$ sites is not fully obeyed. Despite that, this configuration lowers the total energy by about 200 meV/f.u. compared with structure I [Fig. 2(b)] and structure II [Fig. 2(c)], where the $M7$ or $M8$ sites are occupied by Zn atoms.

In order to satisfy the electronic octet rule for the $M3$ sites, we relaxed the condition that the space group is *Cmcm*, i.e., lower crystal symmetry. In the lower symmetry configuration, the $M3$ sites are occupied by Zn atoms, while the 16 Ga atoms are distributed as follows: eight in the $M4$ sites, four in the $M7$ or $M8$ sites, and four Ga atoms occupy other sites. These configurations are shown in Figs. 2(e), 2(h), and 2(i), which substantially lower the total energy. However, we found a clear energy difference between the $M8$ and $M7$ sites. The occupation of the $M7$ sites is about 177 meV/f.u. lower in energy than the occupation of the $M8$ sites by Ga atoms. Therefore, due to the large energy difference, only the $M7$ site is occupied by Ga atoms. Thus, the assumption used by Michiue *et al.* in their XRD analysis that both $M8$ and $M7$ sites are simultaneously occupied by Zn atoms is not supported by our calculations and analysis.

Thus, our calculations indicate clearly that the $M7$ sites are occupied by 4 Ga atoms. However, there are still 12 Ga atoms need to be distributed in the cation sites. Several configurations were calculated in which the 12 Ga atoms were distributed over different sites. We found that the 12 Ga atoms favor four Ga motifs in which the Ga atoms form fivefold trigonal-bipyramidal structures. All configurations containing those Ga motifis have similar energies, i.e., differences of less than 10 meV/f.u. The configurations indicated in Figs. 2(g)–2(i) differ by less than 8 meV/f.u.. Thus, it suggests that the $M9$ positions are simultaneously occupied by Ga and Zn atoms. The 12 Ga atoms form four motifs equally spaced in the unit cell, in which the Ga atoms form trigonal-bipyramidal structures and the Zn atoms are fourfold coordinated with the O atoms. The remaining Zn atoms occupy the remaining four-fold M sites. In the low energy configuration, there are no fivefold Zn atoms in GZO_6. As discussed above, we found that the occupation of the $M7$ sites and the formation of the fivefold trigona-bipyramidal Ga motifs are mainly driven by conservation of the electronic octet rule.

At zero temperature, the predicted occupation of the $M9$ sites by Ga and Zn atoms imply a different space group than *Cmcm*, however, at room temperature, the $M9$ sites might be randomly occupied by Ga and Zn atoms. Furthermore, XRD cannot easily separate between Ga and Zn atoms. Thus, the *Cmcm* space group is consistent with our calculations taking into account a random distribution of Ga and Zn atoms in the $M9$ sites, which can be expected at room temperature due to the small energy difference among those structures, Fig. 2.

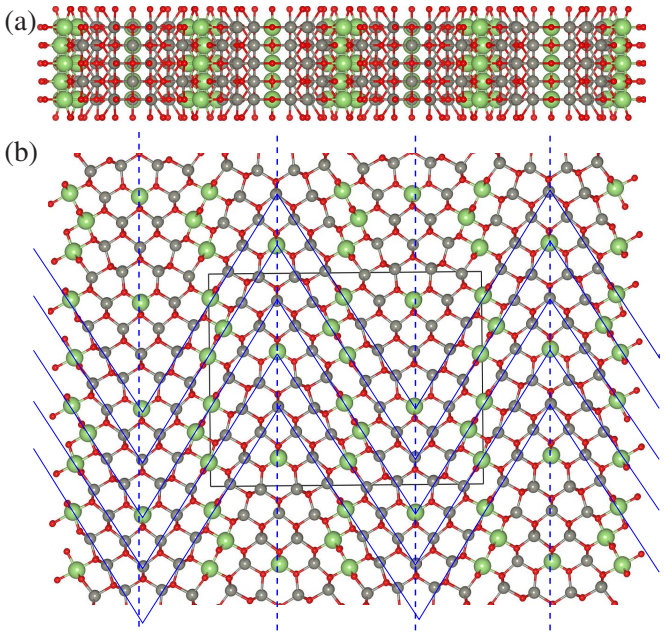

FIG. 3. (Color online) Lowest-energy DFT-PBE orthorhombic GZO_6 structure with the indication of the (a) layered structure and (b) twin-boundary formation. The zigzag blue lines indicate the twin boundary and the vertical blue-dashed lines indicate the position of the mirror symmetry plane. The continuous black lines indicate the underlying orthorhombic unit cell.

The equilibrium lattice parameters of the lowest-energy structure are $a_0=3.28$ Å, $b_0=19.79$ Å, and $c_0=25.45$ Å, which differ by 0.92%, 0.76%, and 2.73% compared with the experimental results ($a_0=3.25$ Å, $b_0=19.64$ Å, and $c_0=24.78$ Å), respectively. Those deviations are within the expected margins of the DFT-PBE framework.[65,66] Thus, our results provide an excellent description of the structural parameters.

1. Natural formation of twin-boundaries in GZO_6

In this section, we will discuss the natural formation of twin boundaries in GZO_6, Fig. 3. The [0001]-ZnO direction can be easily identified in the GZO_6 unit cell in which the majority of ZnO units are aligned, which forms an angle of about 55° with the c axis of the GZO_6 unit cell. The Ga sites are distributed in the (0001)-ZnO planes, in which their local coordination ranges from 4 to 5. Insertion of Ga atoms in the ZnO wurtzite lattice induces the formation of unexpected features. It can be clearly seen that the five-fold Ga atoms in the (0001)-ZnO planes induces a polarity inversion in those planes, i.e., the tetrahedrons formed by ZnO inverts the orientation once a fivefold Ga site is present. Thus, the formation of a twin boundary is to convert the polarity, and hence, preserve the periodicity of the system as indicated in Fig. 3.

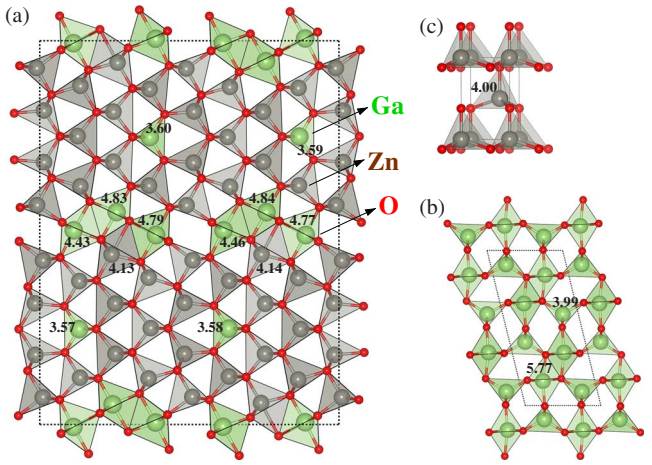

FIG. 4. (Color online) (a) Lowest-energy DFT-PBE orthorhombic GZO_6 structure (8 f.u.). (b) Monoclinic β-Ga_2O_3 structure (4 f.u.). (d) Wurtzite ZnO structure (2 f.u.). The Ga, Zn, and O atoms are indicated by large (green), medium (brown), and small (red) balls. The octahedron (sixfold), trigonal-bipyramidal (fivefold), and tetrahedral (fourfold) polyhedrals are shown. The primitive unit cells are indicated by dashed lines. The ECN is given for the most important polyhedrals. In GZO_6, all Zn atoms without indication of the ECN have an ECN from 3.90 to 4.00.

The twin boundary has an angle of about 106° and it is located between the mirror planes as shown in Fig. 3(b). Thus, the modulations with "V" shape observed by high-resolution analytical transmission electron microscopy[29] (HRTEM) in GZO_9 can be explained by the natural formation of the twin grain boundaries. As noticed for the formation of zigzag modulations in the layered IZO_n compounds,[51] the formation of twin boundaries in GZO_6 (modulations) is mainly due to the existence of Ga atoms with coordination of about 4 and 5. The electronic octet rule plays an important role in the formation of those features. We want to point out that those features present in GZO_6 might also be present in ZnO with high Ga doping concentration, which contributes to the formation of extended defects such as grain boundaries. The presence of such boundaries can also provide sites in which the valence states of the Ga ions (3^+) is satisfied, i.e., they will not contribute electron donors to the lattice. This could be verified experimentally by monitoring the rate of increase in carriers as a function of Ga concentration.

2. *Structure similarities among* $Ga_2O_3(ZnO)_6$, β-Ga_2O_3, *and wurtzite ZnO*

A comparison between crystal structures of GZO_6 and its parent Ga_2O_3 and ZnO compounds can provide insights into the mechanism that drives its formation and stability. Furthermore, it yields a route to generalize the construction of model structures for different compositions. The optimized structures of GZO_6, Ga_2O_3, and ZnO are shown in Fig. 4. To help in our analysis, we will employ the effective coordination concept,[67,68] in which the effective coordination number (ECN) is calculated by taking into account the deviation of bond lengths, l_i, with respect to the weight-averaged bond length, l_{av}, in the polyhedral structures.[69] For example, for l_i smaller (larger) than l_{av}, we obtain a contribution to the ECN larger (smaller) than 1.0 according to the following equations,

$$\mathrm{ECN} = \sum_i exp(1 - (l_i/l_{av})^6), \tag{1}$$

with

$$l_{av} = \frac{\sum_i l_i \exp[1 - (l_i/l_{min})^6]}{\sum_i \exp[1 - (l_i/l_{min})^6]}, \tag{2}$$

where l_{min} is the smallest bond length in the polyhedral. Thus, for a perfect polyhedra, the ECN is equal to the traditional coordination number (CN). Furthermore, we will use the changes in the polyhedral volumes, v_p, as a measure of local transferability among the different structures.[70]

ZnO crystallizes in the wurtzite structure with space group $P6_3mc$, in which the Zn atoms are surrounded by four O atoms and form a near perfect tetrahedron (v_p=4.14 Å^3), i.e., ECN=CN=4.0. The calculated lattice and internal parameters (a_0=3.29 Å, c_0=5.31 Å) are in good agreement with experimental results (a_0=3.25 Å, c_0=5.21 Å).[53] Thus, the Zn-O bond length is 2.00 Å. At room temperature conditions, Ga_2O_3 crystallizes in a monoclinic structure with space group $C2/m$ and 4 f.u. in the primitive unit cell,[71,72] which is known as β-Ga_2O_3, Fig. 4. At high temperature, Ga_2O_3 adopts the corundum Al_2O_3 and bixbyite In_2O_3 structures,[73,74] which have been studied recently by first-principles calculations.[75] We found a_0=12.44 Å, b_0=3.08 Å, c_0=5.88 Å, and β=103.80°, which deviates by 1.85%, 1.32%, 1.41%, −0.03% from the experimental results, a_0=12.21 Å, b_0=3.04 Å, c_0=5.80 Å, and β=103.83°.[71] The internal lattice parameters are summarized in Table I, which show an excellent agreement with the experimental results.[71]

TABLE I. Internal lattice parameters of the β-Ga_2O_3 structure. The numbers in parentheses are experimental results from Ref. 71.

	x	y	z
Ga_1	0.0900(0.0905)	0	0.7947(0.7946)
Ga_2	0.1584(0.1587)	1/2	0.3140(0.3140)
O_1	0.1633(0.1645)	0	0.1093(0.1098)
O_2	0.1736(0.1733)	0	0.5646(0.5632)
O_3	−0.0041(−0.0041)	1/2	0.2566(0.2566)

In contrast to ZnO, β-Ga_2O_3 has a more complex structure. The eight Ga atoms are separated in two groups composed by four slightly distorted octahedron (v_p=10.86 Å^3) and four tetrahedron (v_p=3.31 Å^3) sites, while there are eight three-fold and four four-fold O atoms. In particular, it should be noticed that a pair of octahedrons are surrounded by six tetrahedrons, which can be seen as a basic motif in β-Ga_2O_3. Due to the coordination environment, the polyhedrons are slightly distorted with different bond lengths, e.g., octahedron sites are surrounded by three O at 1.97 Å and

three at 2.04 Å, while there are three O at 1.86 Å and one O at 1.89 Å for the tetrahedron sites. Thus, those distortions give rise to differences between the calculated ECN and the nominal CN. We found ECN=5.77 and 3.99 for the octahedron (CN=6) and tetrahedron (CN=4) sites, respectively. As expected, the electronic octet rule is satisfied for both ZnO and β-Ga_2O_3, and the existence of threefold O atoms is a consequence of the presence of four-fold Ga sites. Due to the coordination, we would expect a slight difference in the local charge between both octahedron and tetrahedron sites. Indeed, we find through Bader analysis that the net charges for the Ga atoms at the tetrahedron and octahedron sites are +1.80 and +1.90, respectively, i.e., a difference of 0.10 between both sites. Thus, we expect a deviation in the charge state of 0.10, which is consistent with previous analysis.[76]

In the orthorhombic GZO_6 structure, the Ga atoms assume a wide range of coordinations. For example, the four Ga atoms in the *M*7 sites have ECN=3.59 and volume of v_p =3.51 Å^3, which is due to the local environment, e.g., two three-fold O atoms at 1.81 Å and two four-fold O atoms at 2.00 Å. Based on the electronic octet rule, the bond lengths difference (about 10%) reflect that Ga donates two electrons to the two threefold O and the remaining one electron is shared by the two four-fold O atoms. Thus, compared with the Ga tetrahedrons in β-Ga_2O_3, the tetrahedrons in GZO_6 have a volume expansion of about 6%. The remaining 12 Ga atoms are distributed in four trigonal-bipyramidal motifs, which are not present in β-Ga_2O_3. We obtained ECN=4.43, 4.78, and 4.82 for the Ga trigonal-bipyramidal structures (v_p=6.45–6.47 Å^3), while ideal trigonal-bipyramidal units have CN=5. For all Zn sites, ECN=3.94–3.99 and v_p =4.00–4.25 Å^3 which differ slightly from the wurtzite ZnO structure. Thus, the introduction of Ga atoms in the wurtzite ZnO lattice in the proportion of one Ga_2O_3 to six ZnO units disturb only slightly the local tetrahedron motifs, however, it introduces extended defects such as the formation of twin-boundaries and polarity inversion. Therefore, for large ZnO to Ga_2O_3 ratio such as n=6, the motifs present in β-Ga_2O_3 are not preserved in the final ternary compound. We would expect that for larger Ga:Zn ratio, more Ga_2O_3 features and less ZnO wurtzite features would be preserved

B. Stability

The stability of the GZO_n compounds with respect to the β-Ga_2O_3 and ZnO compounds can be studied by calculating the respective formation energies, ΔE, i.e.,

$$\Delta E = E_{\text{tot}}^{\text{GZO}_n} - E_{\text{tot}}^{\beta\text{-Ga}_2\text{O}_3} - nE_{\text{tot}}^{\text{ZnO}}, \quad (3)$$

where $E_{\text{tot}}^{\text{system}}$ indicates the total energy per f.u. for the GZO_n, β-Ga_2O_3, and ZnO systems. We found a positive formation energy for GZO_6 of 0.25 eV/f.u., which indicates that GZO_6 is unstable with respect to phase separation at T=0. However, coherent GZO_6 could be stabilized using nonequilibrium epitaxial growth with appropriate substrate.[77]

C. Electronic structure properties

In this section, we will discuss the electron density reorganization upon the multicompound formation using Bader analysis, the electronic density of states, and optical absorption coefficients of GZO_6. In order to gain a better understanding of its electronic structures, we also compared them with those of ZnO and β-Ga_2O_3.

TABLE II. Bader charges, Z_B, given with respect the total valence charge for the ZnO, β-Ga_2O_3, and GZO_6 compounds. The numbers in parentheses indicate the standard coordination number of the respective atoms, i.e., number of O atoms surrounded it.

System	Ga	Zn	O
ZnO		−1.32(4)	+1.32
β-Ga_2O_3	−1.91(6)		+1.25
	−1.80(4)		+1.23
GZO_6	−1.82(5)	−1.31(4)	+1.29
	−1.74(4)	−1.28(5)	+1.23

1. Bader partial charge analysis

In order to obtain insights into the electron density reorganization upon the GZO_6 formation, we calculated the effective Bader charges, Z_B, for ZnO, β-Ga_2O_3, and GZO_6 in their respective lowest-energy structures. The Bader charges, within the Bader volume, are given with respect the total number of valence electrons, i.e., $Z_B=Z_{\text{vol}}-Z_{\text{val}}$. Z_{vol} is the total charge within the Bader volume and Z_{val}=13,12,6 for Ga, Zn, and O. The results are summarized in Table II. Using Bader analysis, we found that Ga and Zn atoms donate electrons to the O atoms in ZnO, β-Ga_2O_3, and GZO_6, which is expected due to the difference in electronegativity. As expected, in β-Ga_2O_3 the two nonequivalent Ga atoms, with different coordination environments, show a difference of about 0.10 electrons in the Bader analysis, which indicates a slight difference in the charge states of both Ga atoms. We found very similar Bader charges for Ga, Zn, and O atoms in the GZO_6 compound. The fourfold Zn atoms GZO_6 have about the same Bader charge (−1.31) as in ZnO (−1.32), while a slightly smaller Bader charge (−1.28) is found for Zn atoms with coordination larger than four. A similar trend is found for the Ga and O atoms as can be seen in Table II. Thus, it is important to notice that quite large changes in the local motifs lead to very slight changes in the Bader analysis, which stresses the importance of well converged calculations in order to study such slightly differences. Therefore, this analysis indicates that the local environments in GZO_6 preserve important electron density features present in the parent compounds.

2. Density of states and band gaps

The total and local density of states (LDOS) are shown in Fig. 5 for the GZO_6, β-Ga_2O_3, and ZnO. The LDOS of the Ga, Zn, and O atoms were obtained by average the LDOS of all respective atoms in the unit cell. The vertical dashed lines indicate the valence-band maximum (VBM). The ZnO LDOS show the well-known features of ZnO, i.e., the VBM consists mostly the O *p* and Zn *d* states.[78] For β-Ga_2O_3 the VBM is dominated by the O *p* state. There are two non-

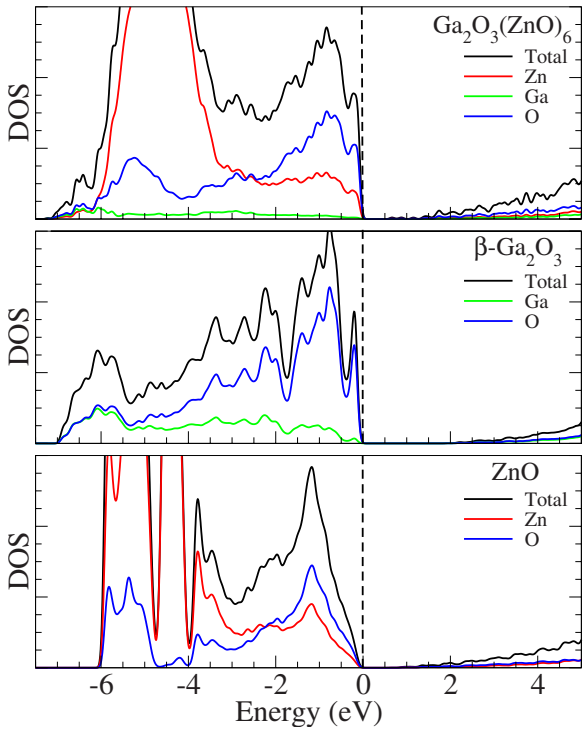

FIG. 5. (Color online) Total and local electronic density of states of ZnO, β-Ga_2O_3, and $Ga_2O_3(ZnO)_6$ in the wurtzite, monoclinic, spinel, and orthorhombic structures.

equivalent Ga atoms in β-Ga_2O_3, in which the Ga atoms are four- and five-fold coordinated. Thus, we would expect that Ga at the two sites would show large differences in their LDOS. However, surprisingly, we found similar LDOS for both Ga environments. This is because despite the coordination is different for the two type of Ga, the oxidation state is similar in both cases due to the presence of threefold O atoms and the satisfaction of the electronic octet rule. Indeed, Bader analysis yields charge states of 2.9+ and 3.1+ for Ga atoms in the tetrahedron and octahedron sites.

The LDOS of GZO_6 shows the main features present in the β-Ga_2O_3 and ZnO compounds. The valence band is dominated by O and Zn states, while there is a very small contribution from the Ga states, which is expected taking into account the concentration of Ga atoms in GZO_6. The Zn *d* states are composed by a broadened peak, which is due to wide range of coordination environments from 3.90 to 4.50 in GZO_6. Furthermore, due to the presence of Ga atoms, we observe a large bandwidth in GZO_6 compared with ZnO.

The DFT-PBE (experimental) fundamental band gaps at the Γ point, E_g, are 0.88, 2.03 (5.2), and 0.73 (3.4 eV) for the GZO_6, β-Ga_2O_3, and ZnO compounds. Thus, our results indicate that the band gap of GZO_6 is dictated by the band gap in ZnO, there is only a marginal increase of 0.15 eV above the host ZnO band gap. This is expected due to the high concentration of ZnO in GZO_6 and the band alignment between ZnO and β-Ga_2O_3. However, due to the well known deficiencies in DFT-PBE, our calculated band gaps are substantially smaller than the experimental results.[65,78]

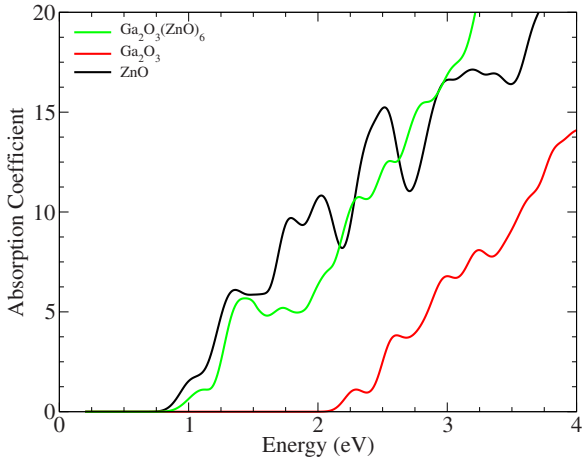

FIG. 6. (Color online) Optical absorption coefficient of ZnO, β-Ga_2O_3, and $Ga_2O_3(ZnO)_6$ in the wurtzite, monoclinic, spinel, and orthorhombic structures.

3. Absorption coefficients

Recent theoretical and experimental studies found that the fundamental and optical band gap of In_2O_3 in the bixbyite structure differs by about 0.80 eV,[79] which plays an important role in explaining the high performance of In_2O_3 as the material of choice for TCO applications. Therefore, similar analysis was performed in this work by calculating the absorption coefficients. The absorption coefficients of GZO_6, β-Ga_2O_3, and ZnO are shown in Fig. 6.

The absorption coefficients, $A_{\alpha\alpha}$, were calculated from the imaginary and real parts of the optical dielectric functions,[80] i.e.,

$$A_{\alpha\alpha} = \frac{\omega\sqrt{2[|\epsilon_{\alpha\alpha}(\omega)| - \mathrm{Re}\ \epsilon_{\alpha\alpha}(\omega)]}}{c}, \tag{4}$$

where ω is the angular frequency of the light, $\epsilon_{\alpha\alpha}$ is the complex dielectric function of polarization $\alpha\alpha$, and c is the speed of light.

The dielectric function (imaginary and real parts) were calculated using the longitudinal pseudopotential approach as implemented in VASP.[81,82] In this approach, the transition matrix elements between the valence and conduction bands are used to derive the imaginary part of the dielectric function, while the real part is obtained from the imaginary part through the Kramers-Kronig relations.[83] In order to obtain consistent and accurate dielectric functions, the sum of occupied and unoccupied states was set to equal the number of valence electrons in the supercell for all calculations.

In contrast to In_2O_3, we found that the fundamental and optical band gaps of GZO_6 are the same, which can be verified by comparing our calculated band gaps with the onset of the nonzero absorption coefficients. As mentioned above, the electronic properties of GZO_6 is dominated by ZnO. It can be seen clearly that the absorption coefficients have similar shape for GZO_6 and ZnO. Thus, in order to obtain large band gaps for GZO, we have to choose GZO with high Ga/Zn ratios such as 1:1 or 2:1.

IV. SUMMARY

In this work, using first-principles methods, we investigated the structure and electronic properties of GZO_6. For comparison, the parent compounds, namely, β-Ga_2O_3 and ZnO were also calculated. We identified a low-energy atomic configuration for the coherent distribution of the Ga and Zn atoms in the GZO_6 structure. Using XRD analysis, Michiue *et al.*[34] suggested that the Ga atoms are located in the *M*4 and *M*9 sites, while the Zn atoms occupy the remaining sites. Michiue *et al.* also suggested that both *M*7 and *M*8 are occupied by Zn atoms, although, due to the short distance between *M*7 and *M*8, the two sites cannot be occupied simultaneously. In this work, we show that the *M*7 site is preferentially occupied by Ga, not by Zn atoms, while the *M*8 site is empty. Therefore, there is no fractional occupation of the *M*7 and *M*8 sites. Furthermore, we found that the remaining 12 Ga atoms in the unit cell form four Ga agglomerates (a motif of four atoms) in which the Ga atoms form trigonal-bipyramidal structures with a wide range of coordinations. Thus, Ga atoms do not distribute uniformly in ZnO matrix, which would be desirable for high Ga doping in ZnO.

We also identified the natural formation of twin boundaries in GZO_6, which can explain the zigzag modulations observed by HRTEM experiments in GZO_n compounds for $n=9$. A consequence of the twin-boundary formation is the polarity inversion of the ZnO tetrahedra within the unit cell. The polarity inversion occurs at the Ga agglomerates, i.e., the existence of the trigonal-bipyramidal sites provide the conditions for the occurrence of the polarity inversion, which have also been observed in IZO_6.[51] Thus, the location of the Ga agglomerates play a very important role in the formation of the polarity inversion, and hence, in the twin-boundary formation. A simple analysis shows that the occupation of the *M*7 site by Ga atoms is driven by the electronic octet rule, which is completely satisfied by Ga atoms, while the occupation by Zn atoms leads to an incomplete electronic distribution in the local motif. Thus, its occupation by Zn atoms leads to higher-energy configurations. It can be noticed that the Ga agglomerates are distributed in the ZnO matrix in such a way that it forms almost layered structures, which plays a role to reduce strain energy and satisfy the electronic octet rule. Finally, we reported the electronic structure properties of GZO_6. We found that the electronic properties, density of states and absorption coefficients of GZO_6, are dictated by the electronic properties of ZnO. Thus, in order to obtain TCOs with higher band gaps than ZnO, low ZnO concentration should be used.

[1] P. P. Edwards, A. Porch, M. O. Jones, D. V. Morgan, and R. M. Perks, Dalton Trans. 2004, 2995.
[2] T. Minami, Semicond. Sci. Technol. **20**, S35 (2005).
[3] A. J. Leenheer, J. D. Perkins, M. F. A. M. van Hest, J. J. Berry, R. P. O'Hayre, and D. S. Ginley, Phys. Rev. B **77**, 115215 (2008).
[4] B. G. Lewis and D. C. Paine, MRS Bull. **25**, 22 (2000).
[5] K. Nomura, H. Ohta, K. Ueda, T. Kamiya, M. Hirano, and H. Hosono, Science **300**, 1269 (2003).
[6] J. F. Wager, Science **300**, 1245 (2003).
[7] K. Nomura, H. Ohta, A. Takagi, T. Kamiya, M. Hirano, and H. Hosono, Nature (London) **432**, 488 (2004).
[8] N. L. Dehuff, E. S. Kettenring, D. Hong, H. Q. Chiang, J. F. Wager, R. L. Hoffman, C.-H. Park, and D. A. Keszler, J. Appl. Phys. **97**, 064505 (2005).
[9] E. M. Fortunato, P. M. C. Barquinha, A. C. M. B. G. Pimentel, A. M. F. Gonçalves, A. J. S. Marques, L. M. N. Pereira, and R. F. P. Martins, Adv. Mater. **17**, 590 (2005).
[10] H.-H. Hsieh and C.-C. Wu, Appl. Phys. Lett. **91**, 013502 (2007).
[11] D.-H. Cho *et al.*, Appl. Phys. Lett. **93**, 142111 (2008).
[12] M. Kimura, T. Nakanishi, K. Nomura, T. Kamiya, and H. Hosono, Appl. Phys. Lett. **92**, 133512 (2008).
[13] H. Lim *et al.*, Appl. Phys. Lett. **93**, 063505 (2008).
[14] N. Nadaud, N. Lequeux, M. Manot, J. José, and T. Roisnel, J. Solid State Chem. **135**, 140 (1998).
[15] J. A. Sans, G. Matínez-Criado, J. Pellicer-Porres, J. F. Sánchez-Royo, and A. Segura, Appl. Phys. Lett. **91**, 221904 (2007).
[16] A. S. Gonçalves, M. R. Davalos, N. Masaki, S. Yanagida, A. Morandeira, J. R. Durrant, J. N. Freitas, and A. F. Nogueira, Dalton Trans. 2008, 1487.
[17] C. Yang, X. M. Li, Y. F. Gu, W. D. Yu, X. D. Gao, and Y. W. Zhang, Appl. Phys. Lett. **93**, 112114 (2008).
[18] S. Yoshioka, F. Oba, R. Huang, I. Tanaka, T. Mizoguchi, and T. Yamamoto, J. Appl. Phys. **103**, 014309 (2008).
[19] H. Hosono, M. Yasukawa, and H. Kawazoe, J. Non-Cryst. Solids **203**, 334 (1996).
[20] B. Kumar, H. Gong, and R. Akkipeddi, J. Appl. Phys. **98**, 073703 (2005).
[21] M. P. Taylor *et al.*, Meas. Sci. Technol. **16**, 90 (2005).
[22] B. Yaglioglu, H. Y. Yeom, R. Beresford, and D. C. Paine, Appl. Phys. Lett. **89**, 062103 (2006).
[23] H.-H. Hsieh, T. Kamiya, K. Nomura, H. Hosono, and C.-C. Wu, Appl. Phys. Lett. **92**, 133503 (2008).
[24] R. J. Cava, J. M. Phillips, J. Kwo, G. A. Thomas, R. B. van Dover, S. A. Carter, J. J. Krajewski, W. F. Peck, Jr., J. H. Marshall, and D. H. Rapkine, Appl. Phys. Lett. **64**, 2071 (1994).
[25] N. Kimizuka, M. Isobe, and M. Nakamura, J. Solid State Chem. **116**, 170 (1995).
[26] D. D. Edwards, T. O. Mason, W. Sinkler, and L. D. Marks, J. Solid State Chem. **140**, 242 (1998).
[27] H. Hiramatsu, W.-S. Seo, and K. Koumoto, Chem. Mater. **10**, 3033 (1998).
[28] T. Moriga, D. D. Edwards, T. O. Mason, G. B. Palmer, K. R. Poeppelmeier, J. L. Schindler, C. R. Kannewurf, and I. Nakabayashi, J. Am. Ceram. Soc. **81**, 1310 (1998).
[29] C. Li, Y. Bando, M. Nakamura, K. Kurashima, and N. Kimizuka, Acta Crystallogr. B **55**, 355 (1999).
[30] C. Li, Y. Bando, M. Nakamura, M. Onoda, and N. Kimizuka, J. Solid State Chem. **139**, 347 (1998).
[31] D. D. Edwards, T. O. Mason, W. Sinkler, L. D. Marks, K. R.

Poeppelmeier, Z. Hu, and J. D. Jorgensen, J. Solid State Chem. **150**, 294 (2000).
[32] J.-S. Park, K.-S. Kim, Y.-G. Park, Y.-G. Mo, H. D. Kim, and H. K. Jeong, Adv. Mater. **20**, A1 (2008).
[33] S. P. Harvey, K. R. Poeppelmeier, and T. O. Mason, J. Am. Ceram. Soc. **91**, 3683 (2008).
[34] Y. Michiue, N. Kimizuka, and Y. Kanke, Acta Crystallogr., Sect. B: Struct. Sci. **64**, 521 (2008).
[35] K.-W. Chang and J.-J. Wu, J. Phys. Chem. B **109**, 13572 (2005).
[36] S. Ju, F. Ishikawa, P. Chen, H.-K. Chang, C. Zhou, Y.-G. Ha, J. Liu, A. Facchetti, T. J. Marks, and D. B. Janes, Appl. Phys. Lett. **92**, 222105 (2008).
[37] W. Zhang, J. Jie, L. Luo, G. Yuan, Z. He, Z. Yao, Z. Chen, C.-S. Lee, W. Zhang, and S.-T. Lee, Appl. Phys. Lett. **93**, 183111 (2008).
[38] X. Zhang, H. Lu, H. Gao, X. Wang, H. Xu, Q. Li, and S. Hark, Cryst. Growth Des. **9**, 364 (2009).
[39] J. J. Berry, D. S. Ginley, and P. E. Burrows, Appl. Phys. Lett. **92**, 193304 (2008).
[40] A. R. Phani, S. Santucci, S. Di Nardo, L. Lozzi, M. Passacantando, P. Picozzi, and C. Cantalini, J. Mater. Sci. **33**, 3969 (1998).
[41] J. S. Kim, H. L. Park, C. M. Chon, H. S. Moon, and T. W. Kim, Solid State Commun. **129**, 163 (2004).
[42] H. Kasper, Z. Anorg. Allg. Chem. **349**, 113 (1967).
[43] P. J. Cannard and R. J. D. Tilley, J. Solid State Chem. **73**, 418 (1988).
[44] M. Nakamura, N. Kimizuka, and T. Mohri, J. Solid State Chem. **93**, 298 (1991).
[45] M. Nakamura, N. Kimizuka, T. Mohri, and M. Isobe, J. Solid State Chem. **105**, 535 (1993).
[46] Y. Yan, S. J. Pennycook, J. Dai, R. P. H. Chang, A. Wang, and T. J. Marks, Appl. Phys. Lett. **73**, 2585 (1998).
[47] T. Moriga, D. R. Kammler, T. O. Mason, G. B. Palmer, and K. R. Poeppelmeier, J. Am. Ceram. Soc. **82**, 2705 (1999).
[48] H. Ohta, K. Nomura, M. Orita, M. Hirano, and K. Ueda, Adv. Funct. Mater. **13**, 139 (2003).
[49] J. E. Medvedeva, Europhys. Lett. **78**, 57004 (2007).
[50] Y. Yan, J. L. F. Da Silva, S.-H. Wei, and M. Al-Jassim, Appl. Phys. Lett. **90**, 261904 (2007).
[51] J. L. F. Da Silva, Y. Yan, and S.-H. Wei, Phys. Rev. Lett. **100**, 255501 (2008).
[52] A. Walsh, J. L. F. Da Silva, Y. Yan, M. M. Al-Jassim, and S.-H. Wei, Phys. Rev. B **79**, 073105 (2009).
[53] C. Kittel, *Introduction to Solid State Physics* (Wiley, New York, 1996).
[54] P. E. Blöchl, Phys. Rev. B **50**, 17953 (1994).
[55] G. Kresse and D. Joubert, Phys. Rev. B **59**, 1758 (1999).
[56] P. Hohenberg and W. Kohn, Phys. Rev. **136**, B864 (1964).
[57] W. Kohn and L. J. Sham, Phys. Rev. **140**, A1133 (1965).
[58] J. P. Perdew, K. Burke, and M. Ernzerhof, Phys. Rev. Lett. **77**, 3865 (1996).
[59] G. Kresse and J. Hafner, Phys. Rev. B **48**, 13115 (1993).
[60] G. Kresse and J. Furthmüller, Phys. Rev. B **54**, 11169 (1996).
[61] G. Henkelman, A. Arnaldsson, and H. Jónsson, Comput. Mater. Sci. **36**, 354 (2006).
[62] E. Sanville, S. D. Kenny, R. Smith, and G. Henkelman, J. Comput. Chem. **28**, 899 (2007).
[63] W. Tang, E. Sanville, and G. Henkelman, J. Phys.: Condens. Matter **21**, 084204 (2009).
[64] M. Isobe, N. Kimizuka, M. Nakamura, and T. Mohri, Acta Crystallogr., Sect. C: Cryst. Struct. Commun. **50**, 332 (1994).
[65] M. Fuchs, J. L. F. Da Silva, C. Stampfl, J. Neugebauer, and M. Scheffler, Phys. Rev. B **65**, 245212 (2002).
[66] J. L. F. Da Silva, S.-H. Wei, J. Zhou, and X. Wu, Appl. Phys. Lett. **91**, 091902 (2007).
[67] R. Hoppe, Angew. Chem. Int. Ed. Engl. **9**, 25 (1970).
[68] R. Hoppe, Z. Kristallogr. **150**, 23 (1979).
[69] K. Momma and F. Izumi, J. Appl. Crystallogr. **41**, 653 (2008).
[70] D. K. Swanson and R. C. Peterson, Canadium Mineralogist **18**, 153 (1980).
[71] J. Åhman, G. Svensson, and H. Albertsson, Acta Crystallogr., Sect. C: Cryst. Struct. Commun. **52**, 1336 (1996).
[72] S. Geller, J. Chem. Phys. **33**, 676 (1960).
[73] R. Roy, V. G. Hill, and E. F. Osborn, J. Am. Chem. Soc. **74**, 719 (1952).
[74] D. M. Giaquinta, W. M. Davis, and H.-C. zur Loye, Acta Crystallogr., Sect. C: Cryst. Struct. Commun. **50**, 5 (1994).
[75] S. Yoshioka, H. Hayashi, A. Kuwabara, F. Oba, K. Matsunaga, and I. Tanaka, J. Phys.: Condens. Matter **19**, 346211 (2007).
[76] R. Hoppe, S. Voigt, H. Glaum, J. Kissel, H. P. Müller, and K. Bernet, J. Less Common Met. **156**, 105 (1989).
[77] S. Froyen, S.-H. Wei, and A. Zunger, Phys. Rev. B **38**, 10124 (1988).
[78] A. Walsh, J. L. F. Da Silva, and S.-H. Wei, Phys. Rev. Lett. **100**, 256401 (2008).
[79] A. Walsh *et al.*, Phys. Rev. Lett. **100**, 167402 (2008).
[80] D. Segev and S.-H. Wei, Phys. Rev. B **71**, 125129 (2005).
[81] B. Adolph, J. Furthmüller, and F. Bechstedt, Phys. Rev. B **63**, 125108 (2001).
[82] M. Gajdoš, K. Hummer, G. Kresse, J. Furthmüller, and F. Bechstedt, Phys. Rev. B **73**, 045112 (2006).
[83] P. Y. Yu and M. Cardona, *Fundamentals of Semiconductors*, 2nd ed. (Spinger-Verlag, Berlin, 1999).